

Review

Base Metal Co-Fired Multilayer Piezoelectrics

Lisheng Gao ^{*}, Hanzheng Guo, Shujun Zhang and Clive A. Randall

Department of Materials Science and Engineering, Materials Research Institute, The Pennsylvania State University, University Park, PA 16802, USA; hug17@psu.edu (H.G.); soz1@psu.edu (S.Z.); car4@psu.edu (C.A.R.)

* Correspondence: lig5167@psu.edu; Tel.: +1-814-441-5190

Academic Editor: Delbert Tesar

Received: 6 January 2016; Accepted: 25 February 2016; Published: 1 March 2016

Abstract: Piezoelectrics have been widely used in different kinds of applications, from the automobile industry to consumer electronics. The novel multilayer piezoelectrics, which are inspired by multilayer ceramic capacitors, not only minimize the size of the functional parts, but also maximize energy efficiency. Development of multilayer piezoelectric devices is at a significant crossroads on the way to achieving low costs, high efficiency, and excellent reliability. Concerning the costs of manufacturing multilayer piezoelectrics, the trend is to replace the costly noble metal internal electrodes with base metal materials. This paper discusses the materials development of metal co-firing and the progress of integrating current base metal chemistries. There are some significant considerations in metal co-firing multilayer piezoelectrics: retaining stoichiometry with volatile Pb and alkaline elements in ceramics, the selection of appropriate sintering agents to lower the sintering temperature with minimum impact on piezoelectric performance, and designing effective binder formulation for low pO₂ burnout to prevent oxidation of Ni and Cu base metal.

Keywords: multilayer actuator; base-metal cofiring; piezoelectrics

1. Introduction

Piezoelectric applications are trending towards miniaturization, better performance, lower energy consumption, being more eco-friendly, higher reliability, and lower cost [1]. The demand for piezoelectric components has been increasing over the years [2,3]. With continued technology development, the piezoelectric business is rapidly expanding in the number and diversity of commercial products. It is estimated that the industrial and consumer piezoelectric business will reach a total of 36 billion USD in 2017, to which actuators would contribute roughly 14 billion USD [4]. Piezoelectric ceramics are becoming popular because of the ease of fabricating devices into different geometries and sizes. Piezoelectrics are experiencing growth in areas such as industrial automation, home automation, and consumer electronics. Currently, the global markets for conventional piezoelectric products are quite mature. There are market predictions of a two-orders-of-magnitude growth of the new piezoelectric products over the next five years [4]. The growth rates of piezoelectric actuators and motors are being driven primarily by automobiles (especially the piezoelectric fuel engine injectors, which are mostly diesel but with recent growth into gasoline injectors), information technology, and biomedical engineering. With the recent scandals regarding diesel emissions, though, there are further opportunities for piezoelectrics, as piezoelectric actuators can provide more sophisticated injection algorithms than the solenoid injectors and provide superior emission control. This is a very complex decision for companies, and those with joint development strategies may be technologically better-positioned to take advantage of the post-scandal era. In view of the global map of piezoelectric products, the robust, growing civilian piezoelectric products have continually diluted the market share of military applications, which were mostly sonar based. Despite the performance, reliability, and market demands,

the piezoelectric industry has been continually suffering from the high costs of precious metal electrodes. Additionally, manufacturing multilayer actuators is different from that of multilayer ceramic capacitors (MLCC), which have industrial standards for size and performance providing a focus for large-scale mass production. Multilayer ceramic actuators do not have standards for production; business relationships and cooperative development in the supply chain, so this diversity creates a more customer-based product. Furthermore, the economic crisis in major palladium producer Russia back in the 1990s drastically increased the market price of palladium, resulting in cost issues to manufacturers for using this metal electrode material [5]. Collectively, an effective strategy to decreasing the costs is to switch the widely used precious metal electrodes to base metal electrodes. Therefore, a reliable base metal co-firing technology would set up a solid foundation for the continually robust market growth in the future through further lowering the manufacturing costs.

2. Applications of Multilayer Piezoelectrics

Multilayer piezoelectrics are widely used in actuators/motors, transformers, and sensors. The multilayer actuators can be utilized in a diesel engine to replace the electromagnetic solenoid valves. A carefully designed multilayer piezoelectric actuator injector and control system can provide a number of attractive advantages over the solenoid system, including, but not limited to, easy starting, high fuel efficiency, and rapid response speed. The response time of the nozzle needle is less than 10^{-4} s. This fast response reduces the fuel delivery rate, thus cutting the energy consumption of the fuel pump. A more sophisticated design of the fuel injector will also increase the efficiency of the diesel combustion engine. For this kind of application, piezoelectric material is required that is elastically stiffer and can charge-discharge quickly. The delicate designs of both injectors and the integrated actuators vary with each case. Specifically, geometry, capacitance, and electromechanical performance all change. All these variations cause the manufacturer to tend to be original equipment manufacturer (OEM) orientated. Other than injectors, the multilayer piezoelectrics are used for haptic applications, airbag sensors, keyless entry systems, and tire pressure monitors. Compared to the traditional electromagnetic-driven actuators/motors or transformers, the energy efficiency of multilayer piezoelectric actuators/motors is independent of the size and geometry. This independence is important because most home or office automation equipment requires tiny driven motors. Meanwhile, such advantages in controlling size offer opportunities to perfectly integrate a multilayer piezoelectric transformer into thin LCDs (liquid crystal displays) to increase the voltage for quick ignition and operation of the fluorescent backlight. Multilayer transformers are also being considered for step-up and step-down transformers in power electronic packages, and also in voltage sensors [6].

3. Multilayer Co-Firing

The conventional single layer disk design and glued stacking design were preliminarily used over an extended period. Those have very limited performance, due to not only the relatively thick ceramic layers and higher drive voltage, but also to the time-consuming polishing step in manufacturing to reach the requirement for applications. However, by using the metal co-fired multilayer structures, the performance of the piezoelectrics is improved through lowering the driving voltage and increasing the overall displacement. As shown in Equation (1), the piezoelectric displacement (ΔL) can be expressed by the number of stacked layers (n) times the normalized strain coefficient (d_{33}^*) and electric field (E).

$$\Delta L = n \cdot d_{33}^* \cdot E \quad (1)$$

The piezoelectric actuators convert electrical energy into mechanical energy so that it can develop usable force. Blocking force is a maximum force that a piezoelectric actuator can generate under electrical load. It is represented in the form of force required to push back an electric field-loaded actuator to its original length. Equation (2) illustrates the relationship between blocking force (F_{max})

and displacement (ΔL); k is the actuator stiffness. The enhanced maximum displacement of a multilayer actuator raises the blocking force, and that improves the mechanical performance.

$$F_{max} = k \cdot \Delta L \quad (2)$$

The multilayer co-fired actuators (MLA) have thinner electrodes, requiring a relatively small driving voltage to obtain the equivalent strain. Despite the performance of the piezoelectric materials, a comprehensive understanding of material processing for multilayer co-fired actuators must address the complexity of co-firing, including optimizing each step of processing to obtain desired microstructures, density, and interaction-free interfaces simultaneously to achieve reliable electromechanical performance. The ceramic powders are dispersed and mixed with binder solution; these solutions contain constituents such as solvents, dispersants, binder polymers, and plasticizers. Various primary binder polymer systems used include materials such as poly(vinyl butyl) (PVB), poly(acrylic alcohol) (PVA), as well as, rarely, poly(propylene carbonate) (PPC). As shown in Figure 1, once a homogeneous ceramic slurry is prepared, it is then fabricated into the ceramic tapes, and metal electrodes are printed. The printed tapes are aligned and stacked together to build up multilayer actuators. The thick-film metal particle electrodes are designed with ceramic fillers to match the thermal profiles of the ceramic tapes to minimize differential shrinkage between the electrode and the tapes. The multilayer structures are binder burned-out and sintered with delicately designed profiles. There are multiple issues to consider for the process engineers, including the formulation of the binder systems, solvent attack resilience of the binder material, thermal expansion mismatch between electrodes and ceramics, sintering environments, and residual carbon after binder removal. Co-firing ceramics with metal electrodes has been challenging for decades. The noble metal electrode multilayer structures are then sintered under ambient air conditions. However, when base metal electrodes are applied, sintering conditions have to be converted from ambient air to reducing atmosphere to protect the metal electrode from oxidation. One of the common methods to obtain low pO_2 atmosphere is mixing H_2 and H_2O [7]. For the reaction $H_{2(g)} + \frac{1}{2}O_{2(g)} = H_{2O(g)}$, the standard Gibbs formation energy is expressed in Equation (3) [8].

$$\Delta G^0 = -247,500 + 55.85T, (298K - 2000K) \quad (3)$$

At the same time, the Gibbs standard formation energy can also be expressed in the form of Equation (4), where R is the gas constant, T is the temperature, and K_p is the equilibrium constant.

$$\Delta G^0 = -RT \ln K_p \quad (4)$$

The K_p can relate to the partial pressure of the H_2O , H_2 , and O_2 as the relation expressed in Equation (5).

$$K_p = \frac{P_{H_2O}}{P_{H_2} \cdot (P_{O_2})^{\frac{1}{2}}} \quad (5)$$

Based on this method, almost any oxygen partial pressure can be obtained in a reducing atmosphere that necessary for controlling oxidation of copper or nickel electrodes.

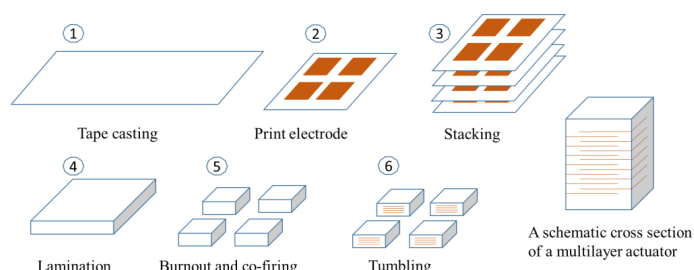


Figure 1. A schematic of processing steps toward multilayer piezoelectrics.

4. Trends of Metal Electrodes

Conventionally, sintering piezoceramics requires very high temperatures, over 1200 °C. At such high temperature, technically, a chemically and physically stable metal, such as Pt, is needed to co-fire with the ceramics. Costs aside, Pt is, of course, an ideal option for co-firing with ceramics; however, commercial applications mean the cost of Pt is too high. On the other hand, with the increased number of stacking layers of the actuators, the cost of electrodes dominates the total cost of the component [9]. Therefore, reduction of the costs of the electrodes would drastically lower the manufacturing costs of multilayer actuators.

Currently, there are two major electrode systems that are widely used commercially: (1) using silver (Ag) and Palladium (Pd) alloy electrodes to sinter in ambient air and (2) using base metal internal electrodes, such as nickel (Ni) or copper (Cu), to co-fire with those non-reducible piezoelectric ceramic materials in a reducing atmosphere. The related properties and price ratio of four common metals are listed in Table 1. Comparing these two systems, the later one can significantly cut the costs of the metal electrode. The Ag/Pd alloy is now widely used in multilayer actuators as internal electrodes, and these are co-fired under an air-sintering condition. Since Ag and Pd form a complete solid solution [10,11], the melting temperature can be varied by altering the composition of the alloy. The Ag-rich alloy is preferred to maintain the high conductivity and control the costs. In contrast, base metal Ni is widely used in BaTiO₃ MLCCs [9]; however, Cu, as an internal electrode material, is still under investigation because of the technical challenges with material processing [12–14]. In this paper, we will review the development of the co-firing technology of three major piezoelectric material systems and demonstrate the recent progress in the base metal co-firing technology of lead-free piezoelectric materials.

Table 1. Important properties of common metal electrode materials.

Metals	Melting Point (°C)	Resistivity ($\times 10^{-8}$ Ω·m)	Young's Modulus (GPa)	Firing Atmosphere	Price Ratio*
Pt	1768	10.5	168	Air	16390
Ag	961	1.6	83	Air	133
Cu	1084	1.7	110	Reducing	1
Ni	1453	6.9	200	Reducing	2
Pd	1552	10.4	121	Air	5930

* The price ratio is based on the price of the investment market, and is also normalized by the factor of mass density due to the consumption amount, based on volume in real applications.

5. Pb(Zr, Ti)O₃

Pb(Zr, Ti)O₃ (PZT) was discovered in the 1950s by Shirane *et al.* [15,16] at the Tokyo Institute of Technology and soon largely replaced BaTiO₃ as a piezoelectric material. Afterward, the Morphotropic Phase Boundary (MPB) was discovered, separating the tetragonal phase and rhombohedral phase, where it is the basic solid solution composition with the highest piezoelectric properties [16]. A more accurate MPB composition was determined at the composition with ~48 mol% of PbTiO₃ and ~52 mol% of PbZrO₃. Due to the arising equivalent energy state, it allows the optimum domain orientation during the poling process [17] for a PZT material with MPB composition, above the ferroelectric transition temperature (T_C) at ~350 °C.

The PZT was initially sintered above 1200 °C to achieve high density. However, it was reported that adding an extra 1 to 2% of excess (over stoichiometry) PbO would lower the sintering temperature. Generation of the PbO liquid phase enables a lower sintering temperature [18,19]. The sintering temperature of PZT was decreased to as low as 900 °C by adding PbO combined with Li₂CO₃ as sintering agents [20,21]. Various sintering agents for lead-based piezoelectric materials, sintering temperatures, and the associated properties are listed in Table 2.

Table 2. Sintering aids, sintering temperatures, and properties of several lead-based piezoelectric materials.

Sintering Aids (% Addition)	Ceramic	Sintering Temperature (°C)	T _c (°C)	ε _r /ε ₀ (RT)	d ₃₃ (pC/N)	d ₃₃ (pm/V)	Reference
LiBiO ₂ (1 wt%) + CuO (0.06 wt%)	PZT	880	-	~1200	-	-	Wang <i>et al.</i> [22]
Li ₂ CO ₃ (0.2 wt%) + PbO (2 wt%)	PZT with Sr, K, Nb	900	360	1200	-	779	Donnelly <i>et al.</i> [20,21,23]
BiFeO ₃ (5 wt%) + Ba(Cu _{0.5} W _{0.5})O ₃ (3 wt%)	PZT with 0.5 wt% MnO ₂	935	290	847	201	-	Kaneko <i>et al.</i> [24]
3ZnO-CuO (3 wt%)	PNN-PZT	900	200	3900	575	-	Ahn <i>et al.</i> [25]
LiBiO ₂ (0.7 wt%)	PMN-PZT and 5% Ba	950	290	~1000		467	Hayashi <i>et al.</i> [26]

5.1. Volatility of Pb

As is well known, lead oxide undergoes a volatilization during heat treatments. When exposed to high temperatures, lead oxide volatilizes into the surrounding atmosphere. The properties of the PZT material can be strongly influenced by the Pb vacancies in the materials. Donnelly *et al.* [27] reported Pb loss while annealing the PZT-0.75%Nb material in ambient air at 700 °C. During the heat treatment, lead (Pb) vacancies and oxygen (O) vacancies were generated at the same time as written in Kröger-Vink notation, which is shown in Equation (6).



The controlling kinetics of the generation of oxygen vacancies and lead vacancies were different. The generation of oxygen vacancies was a bulk diffusion rate-dominated process. The dominating path of Pb volatilization was a result of Pb coupling with the oxygen adsorbed on the surface of the materials [28]. This reaction rate-limited process kinetically controlled the Pb-losing rate of the material. The generation of oxygen vacancies reached equilibrium with the oxygen in the atmosphere, as shown in Equation (7). As a consequence of the high volatilization, the PZT was often sintered with excess PbO or lead sources (PZ) to compensate for the loss of volatile PbO [23,29,30]. Figure 2 shows the ionic conductivity change over time; the gentle slope in the N₂ zone means that the Pb-losing rate is low. This evidence suggested that when air was switched to N₂ with pO₂ < 10⁻⁵ atm, the decreased low pO₂ atmosphere suppressed the volatility of Pb through reducing the contacting chance between environmental O₂ and the materials [28,31], with the losing rate kinetics being controlled from the surface interaction of lead with oxygen at the intermediate temperature ranges of 700 °C to 1000 °C [27].

5.2. Low-Temperature Noble Metal Co-Firing

Co-firing PZT with the relatively cheaper metal electrodes is usually limited by the low melting temperatures of the metals. Compared with Pt, the cheaper Ag/Pd alloy has a lower melting temperature and thus is not able to undergo the high sintering temperature [10]. Various studies on PZT co-firing with different metal electrodes were reported, including the kinetics of sintering and explanations on how co-firing electrodes influence the microstructures, as well as the dielectric and piezoelectric performances. PZT has been successfully co-fired with Ag_{1-x}Pd_x (0 < x < 0.3) electrodes into an interdigitated multilayer PZT piezoelectric structure [32]. Wersing *et al.* [33] reported their work on co-firing PZT with Ag/Pd internal electrodes. Both Pb(Zr_{0.53}Ti_{0.47})O₃ (PZT) and Pb(Ni_{1/3}Nb_{2/3})O₃-PZT (PNN-PZT) multilayer samples were prepared with Ag/Pd (75/25) alloy

electrodes. The multilayer samples were sintered at various temperatures. Moreover, the methodology of lowering the sintering temperatures was engineered through various methods, including optimizing particle sizes, adding various contents of V_2O_3 as a sintering agent, and optimizing the heating rate. It was mentioned that the co-firing temperature had to be lower than $1130\text{ }^{\circ}\text{C}$ to prevent interdiffusion and chemical reactions on the metal-ceramic interfaces. More recently, a study by Caballero *et al.* [34] on Ag/Pd (70/30) co-fired PZT and PNN-PZT further demonstrated the result from Wersing *et al.* [34] by using advanced electron microscopy. Under scanning electron microscopy (SEM), clear electrode-ceramic interfaces were observed, and energy dispersive spectroscopy (EDS) confirmed that there was no Ag/Pd or Pb interdiffusion. In Ag/Pd co-fired multilayer samples, both the EDS data and further transmission electron spectroscopy (TEM) analysis confirmed no interdiffusion of Ag and Pb. The finely controlled sintering work might not induce the Ag or Pb diffusion, but when applied with an electric field, ionized Ag would undergo electromigration along grain boundaries. Electromigration of Ag^+ ions in PZT ceramics causes catastrophic reliability issues in applications. Donnelly *et al.* [35] examined the Ag^+ electromigration in a PZT ceramic applied with high *dc* bias under extreme humidity. After a certain period, the samples exhibited metallic-like conductivity. It revealed that humidities absorbed into the grain boundaries led to the migration of Ag^+ ions under electric fields, where very small amounts of Ag ions evaporate from the electrodes and are distributed into the grain boundaries with excess PbO or other glassy phases associated with the sintering aids. The partial water solubility from the humidity into the glassy phases expedites the migration of Ag^+ ions along the grain boundaries.

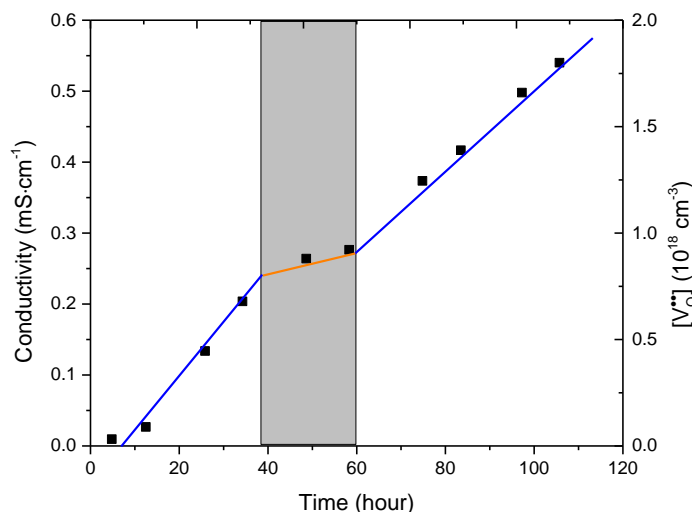


Figure 2. Ionic conductivity in a PZT-0.75%Nb buried capacitor measured over several days at $700\text{ }^{\circ}\text{C}$. Loss of PbO causes the increasing conductivity over time. The increasing oxygen vacancies are due to PbO evaporation: Redrawn from [27].

5.3. Base Metal Co-Firing

Despite Ni being the major base metal electrode choice in BaTiO_3 , paradoxically, PZT is simply not compatible with Ni co-firing because the pO_2 required to retain the metallic Ni electrodes can easily reduce PbO in PZT. As shown in Figure 3, the Ellingham diagram indicates that the NiO is less stable than PbO . Jacob and Saji [36] have conducted experiments on the interaction between Ni/NiO and PbTiO_3 , which was part of the solid solution of the PZT. Their work displayed that direct contact between NiO and PZT did not result in chemical reactions. However, when metallic Ni had direct contact with PbTiO_3 while sintering in either ambient or reducing environments, it reacted with PbTiO_3 and generated a NiTiO_3 phase and a Pb-rich alloy phase, respectively. Further thermodynamic calculations on studying the coexistence between Ni and PbZrO_3 showed similar results. Since the

change of Gibbs potential energy of oxidizing Ni to NiO is lower than that of forming PbO, the direct contact of metallic Ni and PbZrO_3 would also result in the generation of a Pb-rich alloy. These fatal reactions excluded metallic Ni as an appropriate electrode to co-fire with PZT.

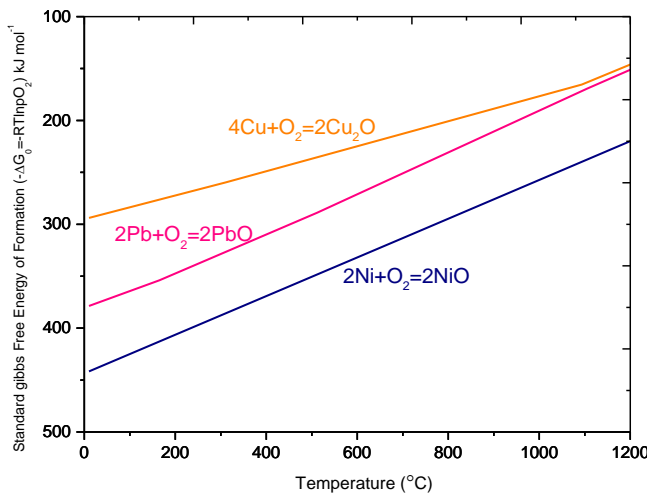


Figure 3. Standard Gibbs formation energy of oxides of Cu, Ni, and Pb, redrawn from [8].

Co-firing the kinetically more readily oxidized copper with PZT is thermodynamically feasible within a narrow pO_2 window. There were published works on co-firing a Cu electrode [37] with PZT-based materials. Takayama *et al.* [38] reported the work on fabricating Cu co-fired PZT-SKN (PZT-Sr($\text{K}_{0.25}\text{Nb}_{0.75}$)O₃) [20,21,23] multilayer actuators. An acrylic binder system was used to lower the burnout temperature, instead of the more widely used PVB; however, this acrylic binder was difficult to handle. The PZT-SKN multilayer actuators with internal glass-coated copper electrodes were burned out in the ambient air at 350 °C. The function of the glass coating on the Cu particles was to prevent the oxidation of Cu during binder burnout in ambient air. Through adding excess PbO (3 wt% and 4 wt%) to the material, the actuators were sintered between 900 °C to 1000 °C under pO_2 of 10^{-12} atm. As a consequence of low pO_2 sintering, reduced piezoelectric constants (both intrinsic and extrinsic) were obtained compared with the air-sintered PZT-SKN. As shown in Figure 4, both gentle slopes and low y-intercepts are obtained from the low pO_2 -sintered PZT samples. The Rayleigh analysis indicates that this special sintering process suppressed both extrinsic and intrinsic piezoelectric properties of the PZT slightly. The SEM micrographs of the cross-section of the multilayer actuators are shown in Figure 5. The results were promising, since there was no Cu diffusion detected under the EDS. A transmission electron microscopy (TEM) micrograph is presented in Figure 6. Figure 6a displays the interface between the Cu electrode and PZT ceramic. Figure 6b shows the vicinity triple points of PZT near the interface. The Cu-free vicinity triple points and grain boundaries verify that there was no Cu diffusion. However, in the Ag or Ag/Pd electrode cases, electrode materials were often observable in these places. Regarding commercial applications, the Cu co-fired PZT had been patented and mass produced by EPCOS, a TDK Group Company [39]. In this EPCOS/TDK product, the Cu co-fired PZT actuators presented a superior performance with a billion switching operations at 170 °C without failures. In contrast, under the same testing conditions, the Ag/Pd co-fired actuators already displayed 50% failures with only 145 million switching operations [40].

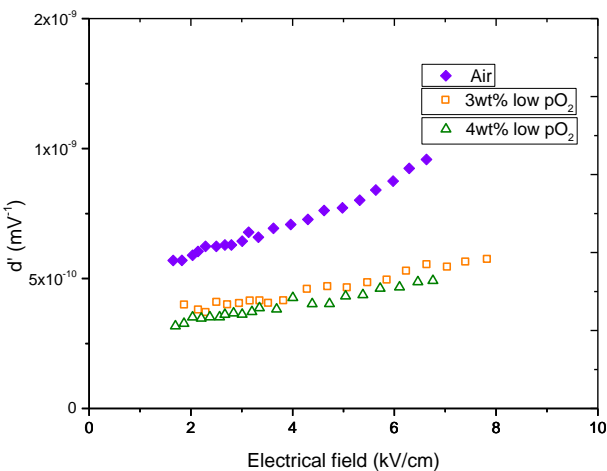


Figure 4. Real piezoelectric coefficients of the sintered PZT-SKN, redrawn from [38].

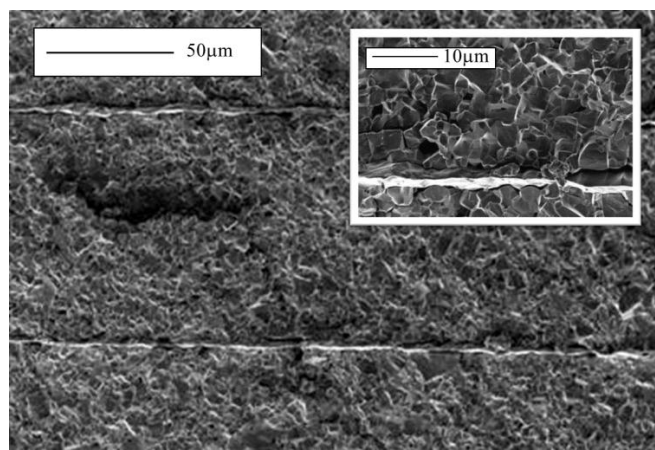


Figure 5. SEM image of multilayer sample with 3 wt% excess PbO [38].

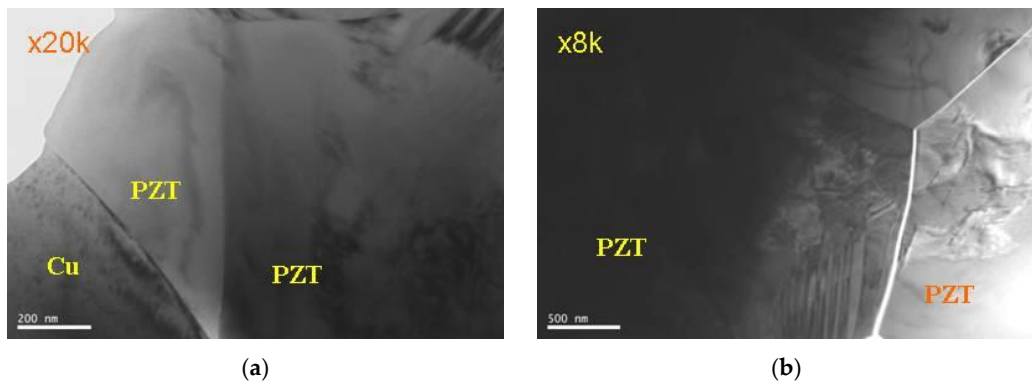


Figure 6. TEM micrograph of (a) Cu-PZT interface, (b) triple points and grain boundaries near electrode [38].

6. BaTiO₃ and Base Metal Co-Firing

As a widely used material for base metal co-fired multilayer capacitors, BaTiO₃ has been intensively studied for use in the base metal co-fired multilayer ceramic capacitors (MLCC) with ultra-thin ceramic layers [9,12,41–47]. The robust success of materials processing led to tremendous work on studying Ni co-fired BaTiO₃, accumulating a rich theoretical and technical basis for future co-firing work toward base metal co-fired multilayer piezoelectrics. Yang *et al.* [48] reported the

interaction between Ni electrodes and the dielectric BaTiO₃ during sintering. Carbonization of binder polymers during burnout generated carbon residues, which dramatically changed the sintering condition through modifying the internal oxygen activity locally on the electrode-ceramic interfaces. The Ni-catalyzed oxidation of residual carbon resulted in the reduction reaction of BaTiO₃ on the interfaces. The reduced Ba and Ti dissolved into the liquid metal phase to form a metal alloy along the ceramic-electrode interface. At the same time, one of the Cu co-fired X7R multilayer capacitors was successfully fabricated by using an acrylic binder system [12]. Utilization of oxide-coated Cu as internal electrodes improved the oxygen resistivity by shielding the atmospheric oxygen from contacting the metallic Cu. Concerning the residual carbon and metal-ceramic interactions, no major issues were noticed. Base metal co-fired BaTiO₃-based dielectric materials have been successfully demonstrated during the past decades, but we still have to face problems from the perspective of ceramic processing, especially in designing an effective binder system that is easy to handle and free of residual carbon.

7. (Na, K)NbO₃

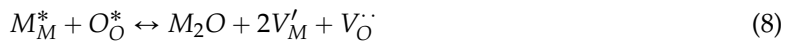
Lead-based Pb(Zr, Ti)O₃ (PZT) and Pb(Mg_{1/3}Nb_{2/3})O₃: PbTiO₃ (PMN-PT) are widely used in commercial applications due to their superior piezoelectric properties. However, concerning the toxicity of lead to both the environment and human beings, the European Union has set a cap on the maximum amount of usage of lead in electronics to 1000 ppm by 2006 and 2011 [49,50]. Though the piezoelectric industries have been continually exempt from the Restriction of Hazardous Substances Directive (RoHS), tremendous effort has been put into studying the lead-free piezoelectric materials to replace the lead-based materials. The perovskite (Na_{0.5}K_{0.5})NbO₃ (NKN) was first reported in 1959 by Egerton and Dillon [51]. Lately, the NKN-based materials have been considered as a potential substitution for PZT, although their performance is still inferior to PZT-based materials. Saito *et al.* [52] reported that textured (Na_{0.5}K_{0.5})NbO₃-based piezoelectric ceramic materials possess comparable piezoelectric properties to PZT. NKN-based materials gained a large spotlight over the other lead-free piezoelectric materials. A series of studies have been conducted by modifying the composition of NKN for better piezoelectric performance and base metal electrode (BME) co-firing. Properties of different modified NKN-based piezoelectric ceramics are presented in Table 3.

Table 3. Properties, additives, and sintering temperatures of several NKN-based piezoelectric ceramics.

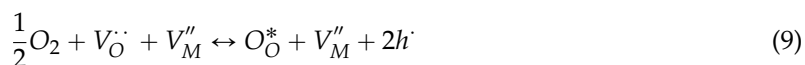
Ceramics	Sintering Aid (mol%)	Sintering Temperature (°C)	T _c (°C)	ε _r /ε ₀ (RT)	d ₃₃ (pC/N)	d ₃₃ * pm/V	Reference
0.99((Na _{0.5} K _{0.5})NbO ₃)-0.01(SrTiO ₃)	-	1100	344	649	90	-	Guo <i>et al.</i> [53]
0.95((Na _{0.5} K _{0.5})NbO ₃)-0.05LiTaO ₃	-	1110	420	570	200	-	Guo <i>et al.</i> [54]
(Na _{0.47} K _{0.47} Li _{0.03})(Nb _{0.8} Ta _{0.2})O ₃	-	~1100	~310	~1000	190	310	E. Hollenstein <i>et al.</i> [55]
0.95[(Na _{0.5} K _{0.5})NbO ₃]-0.05LiTaO ₃	Li ₂ O 1 mol%	1000	-	~450	250	267	Kim <i>et al.</i> [56,57]
(Na _{0.5} K _{0.5})NbO ₃	LiF 5 mol%	1000	456	415	138	210	Kobayashi <i>et al.</i> [58]
0.96(K _{0.5} Na _{0.5})NbO ₃ -0.04CaZrO ₃ +0.03Zr	MnCO ₃ 5 mol%	1080	260	1180	160	360	Kawada <i>et al.</i> [59,60]
0.02(NaF-0.5Nb ₂ O ₅)-0.98 [(Na _{0.5} K _{0.5})(Nb _{0.8} Ta _{0.2})O ₃]	NaF	1200	296	900	140	149	Liu <i>et al.</i> [61]
0.96(K _{0.48} Na _{0.52})(Nb _{0.96} Sb _{0.05})O ₃ -0.04Bi _{0.5} (Na _{0.82} K _{0.18})ZrO ₃	-	1060–1120	227	~2200	490	-	Wang <i>et al.</i> [62]
(K _{0.5} Na _{0.5})NbO ₃ -LiSbO ₃	-	1160	368	1380	265	-	Zhang <i>et al.</i> [63]

7.1. Volatility of Alkaline Elements

Similar to the Pb, alkaline elements in NKN are highly volatile. The NKN materials are haunted by densification and microstructural grain morphology and bimodal grain size issues [64,65]. During the air sintering, the volatile alkaline elements could proceed a volatilization process, as described in the Equation (8), where M represents the alkaline elements.



It is similar to the volatilization path of Pb; the alkaline elements go into the atmosphere via combining with adsorbed atmospheric oxygen at the surface of particles and grains. With the effective zero atmospheric partial pressure of M_2O , vaporization of M_2O would continually proceed until no alkaline elements are left in the material. Generation of oxygen vacancies, though, is coupling with the loss of alkaline elements; such a reaction would reach equilibrium with the atmospheric O_2 following the path as illustrated in Equation (9), which is similar to the case of Pb.



Kobayashi *et al.* [58,66] have demonstrated the work on studying how varying sintering atmosphere affects the microstructures and properties of NKN. The results indicated that once the NKN materials were sintered in the low pO_2 atmosphere, which reduced the possibility of oxygen adsorption onto the surface of the materials, the volatility of alkaline elements decreased. When compared with the air-sintered NKN, the low pO_2 -sintered NKN samples obtained higher electrical resistivity, which further indicated that a higher amount of alkaline elements was retained in the NKN. Similarly, advantages were also noted in the sintering of the end member $NaNbO_3$ [67]. These results were consistent with the first principle calculation that was conducted by Shigemi and Wada [68,69], showing that the formation energy of alkaline vacancies increased when the atmosphere changed from air to low pO_2 .

7.2. Material Modification

Guo *et al.* [53,54] reported the work of $(Na_{0.5}K_{0.5})NbO_3$ materials by developing the dopant system. They doped the $SrTiO_3$ into the NKN system to study how $SrTiO_3$ would influence the piezoelectric properties of NKN [53]. With the highest d_{33} achieved in a non-doped system, the increasing doping amount of $SrTiO_3$ not only caused a drop of d_{33} , but also induced dielectric relaxor behavior. The 4 mol% $SrTiO_3$ has become a critical point separating the orthorhombic phase and tetragonal phase. Such a donor (SrO) and acceptor (TiO_2)-combined doping system solved the poor densification and deliquescence issues of NKN. Following this study, a $LiTaO_3$ -doped NKN system was investigated [54]. The $LaTiO_3$ -doped system gave better piezoelectric properties than that of the $SrTiO_3$ -doped system. The piezoelectric coefficient $d_{33} \sim 200$ pC/N was obtained with 5 mol% dopant. The ferroelectric measurement was carried out with remnant polarization $P_r \sim 9 \mu C/cm^2$ and coercive field ~ 12.5 kV/cm. The Li- and Ta-modified NKN ceramic was further studied by Hollenstein *et al.* [55] through varying the amount of Li and Ta dopant in the composition. The piezoelectric properties were compared between the only Li-doped NKN and both the Li- and Ta-modified NKN system. The 3 mol% Li- and 20 mol% Ta-modified NKN ceramic displayed the best piezoelectric properties of $d_{33}^* \sim 310$ pm/V but possessed a lower Curie temperature of about 310 °C.

7.3. Low-Temperature Co-Firing with Noble Metal

Kim *et al.* [56,57] focused on the Li- and Ta-modified system with just the 5 mol% $LiTaO_3$ -doped NKN material, due to the coupling coefficient reaching its highest value at this composition. A Li_2O sintering agent was used to lower the sintering temperature, in order to meet the temperature requirement of co-firing with the Ag/Pd (70/30) electrode and decrease the volatility of alkaline

elements. The sintering temperature was reduced to 1000 °C. Well-densified samples were achieved with a relative density of 95%. However, this 1 mol% additional sintering aid caused abnormal grain growth because of the change in the critical driving force of grain growth on the faceted interface and grain boundaries. Although adding more than 1 mol% Li₂O, up to 7 mol%, impeded the abnormal grain growth, the considerable sacrifice of d_{33} was observed. The sintered disk bulk samples presented a piezoelectric coefficient of 250 pC/N. A normalized strain coefficient d_{33}^* reached as high as 292 pm/V with Ag/Pd co-fired multilayer samples. The Ag electrode diffused into the ceramic and *vice versa*, forming a thin transition layer, though the Pd could have had some effect on impeding the diffusion slightly [70].

7.4. Low-Temperature Co-Firing with Base Metal

NKN has relatively poor performance compared with PZT-based materials. In order to compete with the PZT-based materials, NKN actuators have to be cheap enough to compensate for their inferior performance. Precious metal electrodes such as the Ag/Pd alloy are not reasonable in view of the costs; at the same time, the diffusion and electromigration issues of Ag could lower the reliability of the devices. Therefore, the spotlight moved to the base metal electrode in seeking low-cost substitutions, as well as looking at the reliability of base metal co-fired NKN piezoelectrics. Kawada *et al.* [59] fabricated the Ni co-fired NKN ceramic (0.96(K_{0.5}Na_{0.5})NbO₃-0.04CaZrO₃+0.03Zr) actuators and displayed a d_{33}^* as high as ~360 pm/V. Figure 7 shows the strain-electric field behavior of the Ni co-fired multilayer actuators. The ceramic tape was fabricated with a poly(vinyl acetate) binder system. The binder was burned out at 400 °C for five hours. Samples were sintered at 1080 °C under pO₂ between 10⁻¹¹ to 10⁻¹⁰ atm for two hours. It was reported that the Ni electrodes have a higher resistivity to electromigration than the Ag/Pd electrode, which is widely used in PZT multilayer actuators [60].

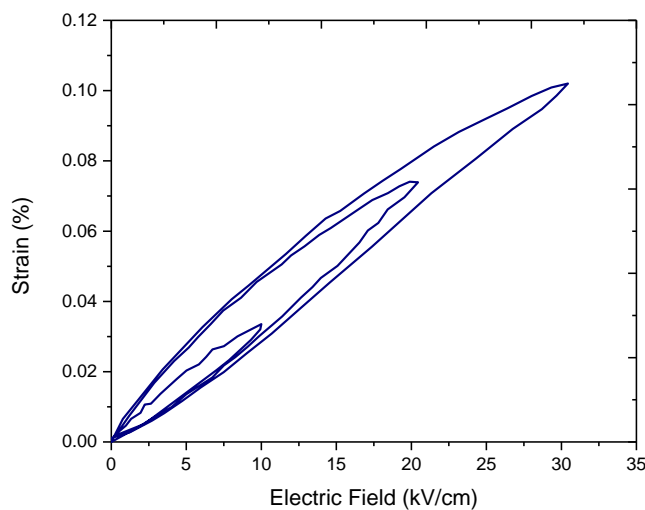


Figure 7. Strain-electric field curve of 0.96(K_{0.5}Na_{0.5})NbO₃-0.04CaZrO₃+0.03Zr multilayer sample with nickel internal electrode, redrawn from [59].

Kobayashi *et al.* [71] conducted parallel experiments on sintering NKN ceramics in both air and low pO₂ atmosphere to understand the differences that low pO₂ sintering made to the properties of NKN. The (Na_{0.5}K_{0.5})NbO₃ with a 5 mol% LiF sintering aid was studied. The results showed that the piezoelectric coefficient of NKN was independent of the sintering atmosphere. As shown in Figure 8, no significant changes in Rayleigh coefficients were observed. The Rayleigh equation is shown in Equation (10), where $d_{initial}$ is the intrinsic piezoelectric coefficient, d is the normalized strain coefficient, and α_d is the Rayleigh coefficient. This phenomenon was quite different from the case of PZT materials [38].

$$d = d_{initial} + \alpha_d E_0 \quad (10)$$

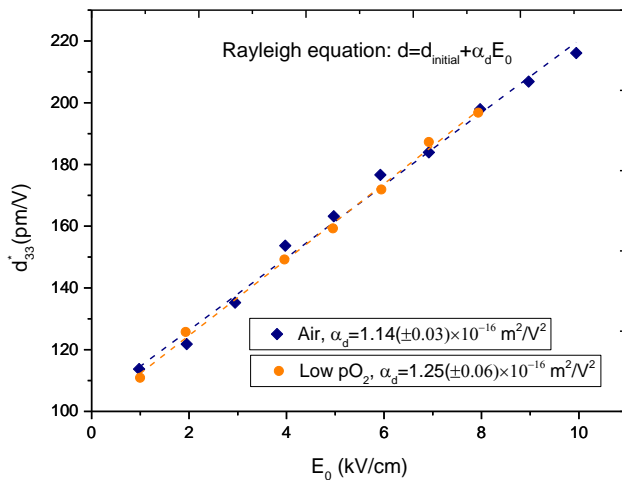


Figure 8. Piezoelectric coefficient d_{33} of a NKN system as a function of applied *ac* field, and linear fitting with the Rayleigh equation, redrawn from [71].

As mentioned, the low pO_2 -sintered NKN had higher resistivity than those that were air-sintered, due to the suppressed volatility of alkaline elements in low pO_2 . Another advantage was that the NKN ceramic sintered in the low pO_2 atmosphere obtained higher density (95% of theoretical density) than those sintered in the air (91% dense) at the same temperature with the same dwelling time. Afterward, further study on fabricating Ni co-fired multilayer NKN actuators was done.

Kobayashi *et al.* [58,66] used the same NKN [71], then fabricated prototype multilayer actuators with Ni internal electrodes. The PVB-formed tapes were printed with a layer of Ni electrodes to prepare the multilayer actuators. The multilayer actuators were burned out at 270 °C for 12 h in N_2 atmosphere. There were no observable macroscopic defects, pores, or delaminations, which were common issues causing low reliability in multilayer actuators. Furthermore, no Ni interdiffusion was detected along the interfaces. Moreover, the Ni electrode did not affect the microstructure of NKN, unlike the alloy formation in the Ni co-fired $BaTiO_3$ system due to the reduction of $BaTiO_3$ by residual carbon. The alloy-free electrode-ceramic interfaces in Ni co-fired NKN multilayer actuators suggested the feature of working against the reduction of NKN. The following year, a $NaF-Nb_2O_5$ flux-doped NKN was reported by Liu *et al.* [61,72] for multilayer actuator applications. The 0.02($NaF_{0.5}Nb_2O_5$)-(0.98)[($Na_{0.5}K_{0.5}$) $(Nb_{0.8}Ta_{0.2})O_3$] was synthesized and then used to fabricate Ni co-fired multilayer actuators. Similar to the majority of the reported work, a PVB binder was used. The binder burnout was performed at 270 °C for 12 h in the air. The multilayer actuators were sintered in a low pO_2 of 10^{-10} atm at 1150 °C for 2 h, and then further reoxidized at 850 °C in a pO_2 of 10^{-7} atm for eight hours. The piezoelectric performance was excellent compared with other lead-free piezoelectric materials; up to 385 pm/V of d_{33}^* was achieved. As a lead-free piezoelectric ceramic, NKN is promising for the future exploration of BME co-firing.

8. $Bi_{0.5}Na_{0.5}TiO_3$

$Bi_{0.5}Na_{0.5}TiO_3$ (NBT)-based lead-free piezoelectric materials drew attention because of their moderate piezoelectric properties. The Ag/Pd co-fired NBT has already been fabricated and reported with reasonable performance and reliability by Sapper *et al.* [73]. Due to the increasing interest in base metal co-firing, recently Safari and his coworkers reported on co-firing 0.88($Bi_{0.5}Na_{0.5}TiO_3$)-0.08($Bi_{0.5}K_{0.5}TiO_3$)-0.04($BaTiO_3$) (BNT-BKT-BT) with metallic Cu [74]. The NBT-based piezoelectric ceramic disks were sintered in both air and low pO_2 atmosphere. The comparison has been made on samples sintered under different conditions. Neither sintering agents nor sintering atmospheres had significant influence on piezoelectric properties; similar piezoelectric properties were obtained. The Cu electrode was pressed between two already burned-out ceramic powder disks. The co-fired

samples showed a d_{33} of 77 pC/N, which was lower than the simple disk sample, having a d_{33} of ~160 pC/N. Collectively, the study presented that this NBT material was compatible for Cu co-firing; further exploration on microstructures and the interdiffusion process is needed.

9. Binder Materials

In view of the work we summarized here, we only saw a couple of works on co-firing Cu with piezoelectric ceramics. Those foreseeable challenges became roadblocks when co-firing involved metallic Cu; Cu is more readily oxidized and has a low melting temperature. Although the glass-coated copper can prevent Cu from oxidation, the influence of the glass coating on Cu particles may introduce contamination and sacrifice of the dielectric and piezoelectric performances. Therefore, a direct solution is to provide a binder system that can be cleanly burned off at low temperature and in a protective atmosphere. The traditional PVB has been widely used in both Ag/Pd and Ni co-fired multilayer actuators, due to the relatively higher oxidation temperature of these metals. Collectively, the binder system in the previous study was usually burned off in ambient air up to 400 °C. This temperature already exceeds the maximum temperature of retaining the metallic state of both Ni and Cu, though Ni electrodes are relatively feasible for burnout up to 300 °C. To effectively prevent Ni and Cu from oxidation, clean burnout has to be achieved at either a reasonably low temperature or in a low pO₂ atmosphere. With the conventional PVB binder system, although well developed, clean burnout of PVB has never been reported at low temperatures. Masia *et al.* [75] reported that the amount of carbon residues of PVB varied with different ceramics. It was revealed, as a matter of fact, that usually at least 500 °C was needed for burnout due to the high activation energy of degradation [76,77]. Salam *et al.* [78] have studied the burnout behavior of PVB, serving as a binder of thermoelectric green tapes, in different kinds of atmosphere up to 450 °C. The results showed that PVB left residues in all conditions. A burnout conducted in ambient air at 450 °C showed that 19.3% of PVB was not removed. In this work, the fraction percentage of PVB left was estimated to be 2% at 600 °C and 1% between 700 °C to 800 °C. While burning out in N₂, the pyrolysis could take place and convert the PVB into carbonaceous char. Breakdown char usually requires higher temperatures than breakdown polymer. It was realized that even at 1000 °C, an appreciable amount of residual carbon could still exist under the N₂ condition [79].

Poly(propylene carbonate) (PPC) has been also studied as a potential binder polymer [80]. It was found that PPC can be cleanly burned out in both air and N₂ at relatively low temperatures. There was no detectable residue left after burnout. Unlike the PVB system, the burnout of PPC followed the depolymerization path to form a propylene carbonate monomer rather than pyrolysis of the polymer into char. The propylene carbonate vaporized without leaving residual carbon. The authors considered that lack of successful formulation of the PPC binder system hindered the utilization of PPC as a successful binder for ceramics.

10. Recent Progress on Cu Co-Fired NKN

Recently, our group successfully fabricated prototype multilayer actuators through co-firing Cu metal electrodes with NKN ceramic [81]. We used the Li- and Ta-modified NKN, which was kindly provided by PI Ceramic. A new poly(propylene carbonate) (PPC) binder was used. The advantage of PPC is that it can be cleanly burned off in reducing atmosphere. The prototype samples were sintered at 1050 °C under a pO₂ of 10⁻¹² atm for one hour, then further annealed at 1000 °C for another hour to allow grain growth. After that, the samples were reoxidized at 850 °C under a pO₂ of 10⁻⁵ atm for 12 h. Microstructures were compared between the low pO₂-sintered, and air-sintered pellets. The SEM surface micrographs are shown in Figure 9. Both samples were sintered at 1050 °C for 1 h. The samples sintered in low pO₂ showed a higher homogeneity of grain size with minimized abnormal growth (Figure 9a). However, lower homogeneity (Figure 9b) was obtained in air-sintered NKN ceramic with a certain amount of abnormal grain growth. Both of them have well-faceted grains.

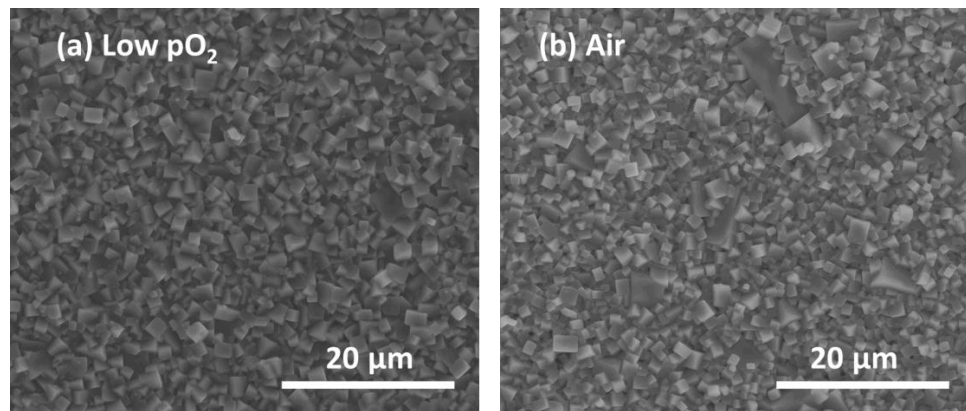


Figure 9. Surface micrograph of (a) low pO_2 -sintered and (b) air-sintered pellets at 1050 °C for 1 h.

A 96% dense NKN ceramic was achieved from sintering plain tapes. The surface SEM micrograph (Figure 10) displayed well-faceted grains (Figure 10a) on the surface of the multilayer co-fired samples. The cross-section is shown in Figure 10b. The internal Cu electrode was continuous and unoxidized. EDS line scan data (Figure 10c) indicated that there was no residual carbon and Cu interdiffusion between Cu electrodes and the NKN ceramic. The microstructure was further studied by TEM (Figure 11a,b); the micrographs were taken along the <001> direction. An atomistically sharp interface between the Cu electrode and ceramic was observed (Figure 11c,d). There was no residual carbon, alloy formation, or CuO in the co-fired multilayer samples under TEM. The dielectric constant was 830, with a low dielectric loss of 3.6%. The co-fired multilayer actuators displayed a Curie temperature (T_c) of ~330 °C. The classic ferroelectric switching (Figure 12) was induced with minimal contribution from space charge and conduction [82], and a coercive field (E_c) of 10.9 kV/cm with a remanent polarization of 22.1 μ C/cm² was obtained. The normalized strain d_{33}^* was 220 pm/V (Figure 13), due to the fact that the interdigitated electrodes would have some clamping effect on the piezoelectric performance. The results are summarized in Table 4. Collectively, the data indicated that the Cu electrode is suitable and attractive for co-firing with NKN.

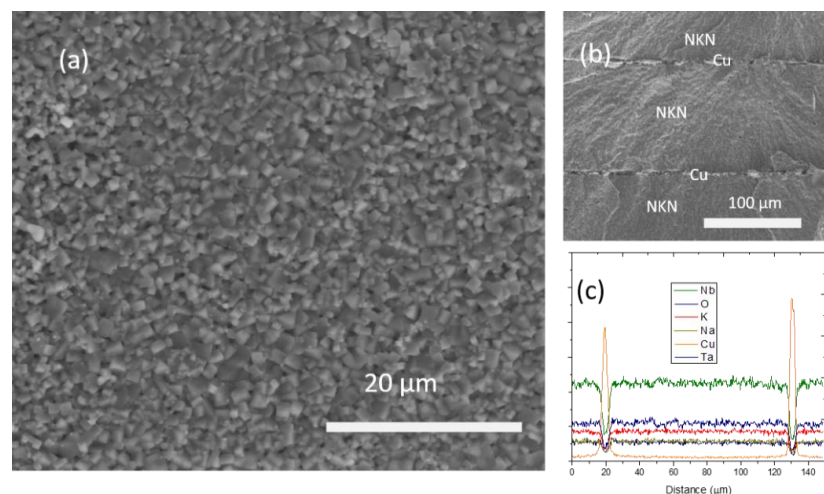


Figure 10. SEM Micrograph on (a) surface, (b) cross-section of Cu co-fired actuator, (c) EDS line scan on the cross-section of Cu co-fired actuator.

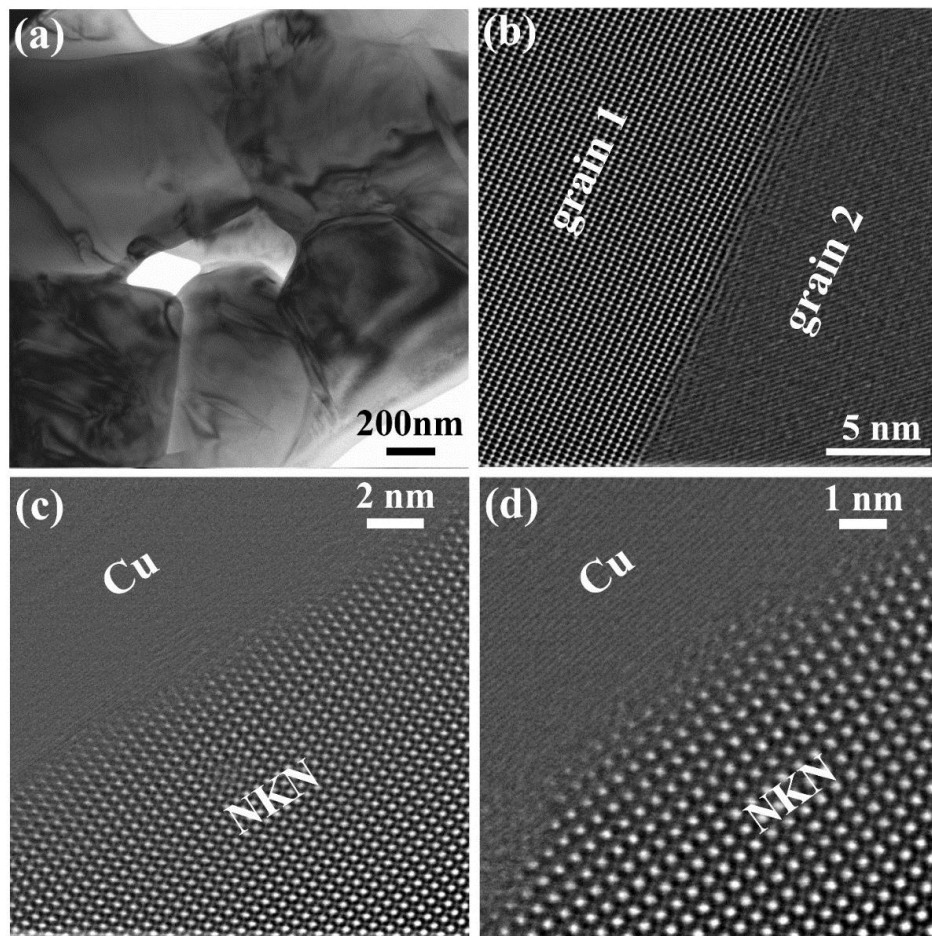


Figure 11. Cu-NKN MLCC (sintered at 1050 °C). (a) The typical TEM micrograph of the grains; (b,c,d) Atomistic STEM images of the grain boundary and Cu/NKN interface, respectively.

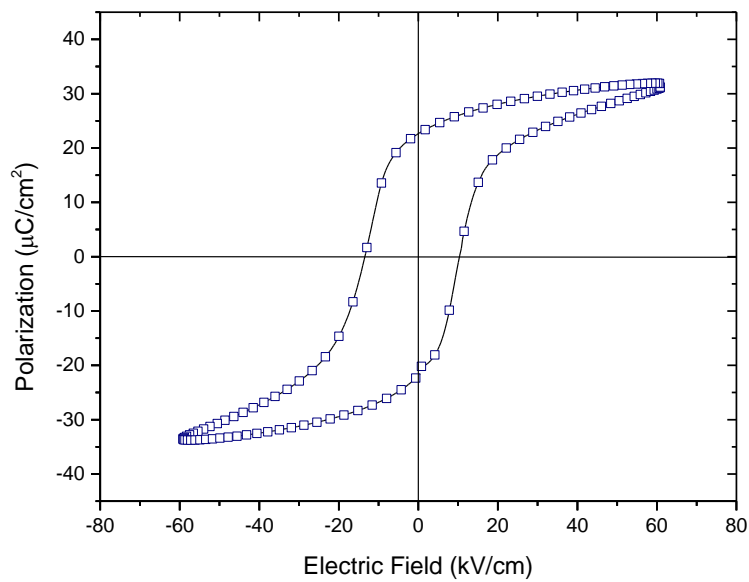


Figure 12. Ferroelectric hysteresis loop of Cu co-fired NKN actuator.

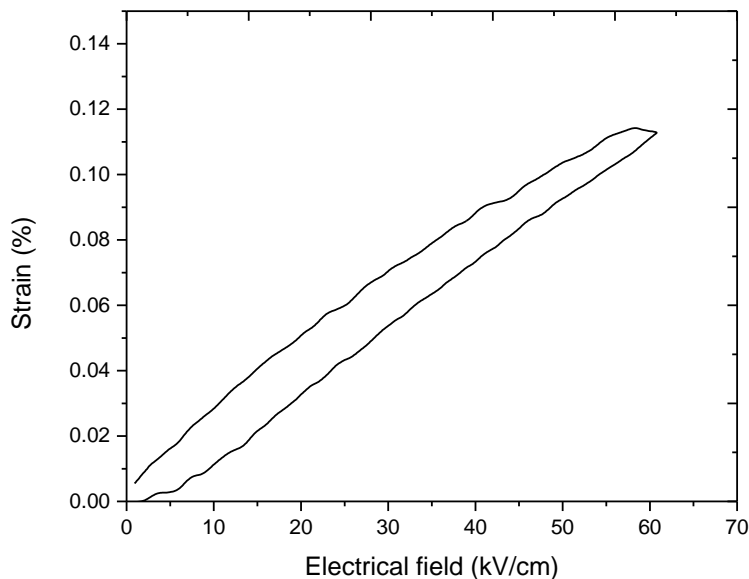


Figure 13. Unipolar electric field–induced strain of Cu Co-fired NKN sample.

Table 4. Values of electrical properties of Cu co-sintered NKN ceramics.

T _c (°C)	ε _r (1 kHz)	d ₃₃ * (pm/V) @ 20 kV/cm	Tan δ (1 kHz)	E _c (kV/cm)	P _r (μC/cm ²)
330	830	220	0.036	10.9	22.1

11. Summary

Recent progress on co-firing Ag/Pd, Ni, and Cu metal electrodes with both PZT and lead-free piezoelectric ceramics was presented. The sinterability of the piezoelectric ceramics was successfully improved via using sintering agents. The effects and mechanisms of adding sintering agents were carefully investigated. It was found that liquid phase sintering significantly lowered the sintering temperatures, thus widening the choices of metal electrode materials.

The volatility of Pb and alkaline elements can be suppressed through sintering in a reduced atmosphere. It was confirmed that the low pO₂–sintered samples showed higher resistivity than the air-sintered ones. The dominating path of losing volatile elements underwent coupling with surface-adsorbed oxygen. Therefore, reducing the pO₂ in the atmosphere consequently cut the chances of contact between the volatile elements and atmospheric oxygen, thereby retaining the volatile elements while sintering.

Interdiffusion of metal electrodes was investigated. The Ag/Pd internal electrode faced both diffusion during sintering and electromigration under electrical load; both resulted in the drop of reliability and lifespan of the piezoelectric applications. Both experimental and calculated results showed that PZT was intrinsically incompatible with metallic Ni electrodes, yet was eligible to co-fire with Cu internal electrodes. The Cu co-fired PZT displayed higher reliability than the Ag/Pd co-fired PZT. The Ni co-fired NKN displayed under-detectable interdiffusion along the electrode-ceramic interfaces and good electromigration resistivity.

The major roadblock toward base metal co-firing was the binder system. While burning out in the low pO₂ condition, the PVB binder could undergo a pyrolysis process, thus leaving carbon residues. However, burning out PPC polymer in the low pO₂ atmosphere follows depolymerization, generating monomers. Such a feature made it a better binder polymer for low pO₂ burnout.

Until very recently, our group utilized the PPC binder and successfully fabricated Cu co-fired prototyped NKN multilayer actuators. The whole heat treatment was conducted under low pO₂

atmosphere. There was no detectable residual carbon, interdiffusion, or alloy formation. Such success could give a general direction for future base metal co-firing investigations. Collectively, base metal (especially Cu) co-firing is largely unexplored; further deep investigations of the binder formulations, burnout conditions, and sintering profiles to realize highly reliable multilayer piezoelectrics are required. Some important information and facts are summarized in Table 5 shown below.

Table 5. Summary of important findings and progress on base metal co-firing for major piezoelectrics.

Materials	Incompatible Metal Electrode	Future Trend of Metal Electrodes	Challenges	Progress on Base-Metal Co-Firing
PZT	Ni	Cu	Binder, pO ₂ control	Production in EPCOS/TDK [40]
NBT	-	Cu	Binder burnout	Pressed Cu with ceramic pellets [74]
NKN	-	Cu	Binder burnout	Cu co-fired prototyped multilayer actuators [81]

Acknowledgments: The authors want to thank Amanda Baker, Steve Perini, and Jeff Long for their dedicated work on managing the lab affairs. Thanks to the Materials Characterization Laboratory (MCL) and Ke Wang for his assistance on TEM. The authors also want to thank PI Ceramics for providing the high-quality NKN ceramic powders. This material is based upon work supported in part by the National Science Foundation, as part of the Center of Dielectrics and Piezoelectrics under Grant No. IIP-1361571.

Author Contributions: C.A.R. and S.Z. conceived and designed the experiments; H.G. provided TEM micrographs; L.G. integrated information and wrote the paper.

Conflicts of Interest: The authors declare no conflict of interest.

References

- Randall, C.A.; Kelnberger, A.; Yang, G.Y.; Eitel, R.E.; Shrout, T.R. High Strain Piezoelectric Multilayer Actuators—A Material Science and Engineering Challenge. *J. Electroceramics* **2005**, *14*, 177–191. [[CrossRef](#)]
- Uchino, K.; Takahashi, S. Multilayer Ceramic Actuators. *Curr. Opin. Solid State Mater. Sci.* **1996**, *1*, 698–705. [[CrossRef](#)]
- Uchino, K. *Ferroelectric Devices*, 2nd ed.; CRC Press: Boca Raton, FL, USA, 2009.
- Abraham, T. Expanding Markets for Piezoelectrics. Available online: <http://www.ceramicindustry.com/articles/93845-expanding-markets-for-piezoelectrics> (accessed on 22 October 2015).
- Uchino, K. *Entrepreneurship for Engineers*; CRC Press: Boca Raton, FL, USA, 2009.
- Knowles, G.J.; Bradley, W.M.; Bird, R. Galvanic Isolated Ceramic Based Voltage Sensors. WO2015153,798 A1, 8 October 2015.
- Imanaka, Y. *Multilayered Low Temperature Cofired Ceramics (LTCC) Technology*; Springer Science & Business Media: New York, NY, USA, 2005.
- Gaskell, D.R. *Introduction to the Thermodynamics of Materials*, 5th ed.; CRC Taylor & Francis Group, LLC: New York, NY, USA, 2008.
- Kishi, H.; Mizuno, Y.; Chazono, H. Base-Metal Electrode-Multilayer Ceramic Capacitors: Past, Present and Future Perspectives. *Jpn. J. Appl. Phys.* **2003**, *42*, 1–15. [[CrossRef](#)]
- Karakaya, I.; Thompson, W.T. The Ag-Pd (Silver-Palladium) System. *Bull. Alloy Phase Diagrams* **1988**, *9*, 237–243. [[CrossRef](#)]
- Wang, S.F.; Dougherty, J.P.; Huebner, W.; Pepin, J.G. Silver-Palladium Thick-Film Conductors. *J. Am. Ceram. Soc.* **1994**, *77*, 3051. [[CrossRef](#)]
- Song, T.; Randall, C.A. Copper Cofire X7R Dielectrics and Multilayer Capacitors Based on Zinc Borate Fluxed Barium Titanate Ceramic. *J. Electroceramics* **2003**, *10*, 39–46. [[CrossRef](#)]
- Yonezawa, T.; Takeoka, S.; Kishi, H.; Ida, K.; Tomonari, M. The Preparation of Copper Fine Particle Paste and its Application as the Inner Electrode Material of a Multilayered Ceramic Capacitor. *Nanotechnology* **2008**, *19*, 145706. [[CrossRef](#)] [[PubMed](#)]

14. Takeoka, S.; Mizuno, Y. Effect of Internal Electrode Materials in Multilayer Ceramic Capacitors on Electrical Properties. *Jpn. J. Appl. Phys.* **2011**, *50*, 1–6. [[CrossRef](#)]
15. Shirane, G.; Takeda, A. Phase Transitions in Solid Solutions of PbZrO₃ and PbTiO₃ (I) Small Concentrations of PbTiO₃. *J. Phys. Soc. Jpn* **1952**, *7*, 5–11. [[CrossRef](#)]
16. Shirane, G.; Suzuki, K.; Takeda, A. Phase Transitions in Solid Solutions of PbZrO₃ and PbTiO₃ (II) X-ray Study. *J. Phys. Soc. Jpn* **1952**, *7*, 12–18. [[CrossRef](#)]
17. Jaffe, B.; Cook, W.R. *Piezoelectric Ceramic*, 1st ed.; Academic Press: London, UK, 1971.
18. Kingon, A.I.; Clark, J.B. Sintering of PZT Ceramics: II, Effect of PbO Content on Densification Kinetics. *J. Am. Ceram. Soc.* **1983**, *66*, 256–260. [[CrossRef](#)]
19. Holman, R.L.; Fulrath, R.M. Intrinsic Nonstoichiometry in Single-Phase Pb(Zr_{0.5}Ti_{0.5})O₃. *J. Am. Ceram. Soc.* **1972**, *55*, 192–194. [[CrossRef](#)]
20. Donnelly, N.J.; Shrout, T.R.; Randall, C.A. Properties of (1-x)PZT-xSKN Ceramics Sintered at Low Temperature Using Li₂CO₃. *J. Am. Ceram. Soc.* **2008**, *91*, 2182–2188. [[CrossRef](#)]
21. Donnelly, N.J.; Shrout, T.R.; Randall, C.A. The Role of Li₂CO₃ and PbO in the Low-Temperature Sintering of Sr, K, Nb (SKN)-Doped PZT. *J. Am. Ceram. Soc.* **2009**, *92*, 1203–1207. [[CrossRef](#)]
22. Wang, X.X.; Murakami, K.; Sugiyama, O.; Kaneko, S. Piezoelectric Properties, Densification Behavior and Microstructural Evolution of Low Temperature Sintered PZT Ceramics with Sintering Aids. *J. Eur. Ceram. Soc.* **2001**, *21*, 1367–1370. [[CrossRef](#)]
23. Donnelly, N.J.; Shrout, T.R.; Randall, C.A. Addition of a Sr, K, Nb (SKN) Combination to PZT(53/47) for High Strain Applications. *J. Am. Ceram. Soc.* **2007**, *90*, 490–495. [[CrossRef](#)]
24. Kaneko, S.; Dong, D.; Murakami, K. Effect of Simultaneous Addition of BiFeO₃ and Ba(Cu_{0.5}W_{0.5})O₃ on Lowering of Sintering Temperature of Pb(Zr,Ti)O₃ Ceramics. *J. Am. Ceram. Soc.* **1998**, *81*, 1013–1018. [[CrossRef](#)]
25. Ahn, C.W.; Nahm, S.; Ryu, J.; Uchino, K.; Yoon, S.J.; Jung, S.J.; Song, J.S. Effects of CuO and ZnO Additives on Sintering Temperature and Piezoelectric Properties of 0.41Pb(Ni_{1/3}Nb_{2/3})O₃-0.36PbTiO₃-0.23PbZrO₃ Ceramics. *Jpn. J. Appl. Phys.* **2004**, *43*, 205–210. [[CrossRef](#)]
26. Hayashi, T.; Hasegawa, T. Piezoelectric Properties of Low-temperature Sintered Pb_{0.95}Ba_{0.05}[(Mg_{1/3}Nb_{2/3})_{0.125}Zr_{0.445}Ti_{0.43}]O₃ Ceramics with Chemically-added LiBiO₂ Sintering Aid. *J. Eur. Ceram. Soc.* **2005**, *25*, 2437–2441. [[CrossRef](#)]
27. Donnelly, N.J.; Randall, C.A. Impedance Spectroscopy of PZT Ceramics—Measuring Diffusion Coefficients, Mixed Conduction, and Pb Loss. *IEEE Trans. Ultrason. Ferroelectr. Freq. Control* **2012**, *59*, 1883–1887. [[CrossRef](#)] [[PubMed](#)]
28. Yoshida, T.; Nagasaka, T.; Hino, M. Effect of Oxygen on the Evaporation Rate of Lead from Liquid Copper under Reduced Pressure. *ISIJ Int.* **2001**, *41*, 706–715. [[CrossRef](#)]
29. Helke, G.; Seifert, S.; Cho, S.-J. Phenomenological and Structural Properties of Piezoelectric Ceramics Based on xPb(Zr,Ti)O₃-(1-x)Sr(K_{0.25}Nb_{0.75})O₃ (PZT/SKN) Solid Solutions. *J. Eur. Ceram. Soc.* **1999**, *19*, 1265–1268. [[CrossRef](#)]
30. Atkin, R.B.; Fulrath, R.M. Point Defects and Sintering of Lead Zirconate-Titanate. *J. Am. Ceram. Soc.* **1971**, *54*, 265–270. [[CrossRef](#)]
31. Donnelly, N.J.; Randall, C.A. Pb Loss in Pb(Zr,Ti)O₃ Ceramics Observed by *in Situ* Ionic Conductivity Measurements. *J. Appl. Phys.* **2011**, *109*, 104107. [[CrossRef](#)]
32. Uchino, K.; Nomura, S.; Cross, L.E.; Newnham, R.E.; Jang, S.J. Electrostrictive Effect in Perovskites and Its Transducer Applications. *J. Mater. Sci.* **1981**, *16*, 569–578. [[CrossRef](#)]
33. Wersing, W.; Wahl, H.; Schnöller, M. PZT-based Multilayer Piezoelectric Ceramics with AgPd-Internal Electrodes. *Ferroelectrics* **1988**, *87*, 271–294. [[CrossRef](#)]
34. Caballero, A.C.; Nieto, E.; Duran, P.; Moure, C.; Kosec, M.; Samardzija, Z.; Drazig, G. Ceramic-Electrode Interaction in PZT and PNN-PZT Multilayer Piezoelectric Ceramics with AG/PD 70/30 Inner Electrode. *J. Mater. Sci.* **1997**, *32*, 3257–3262. [[CrossRef](#)]
35. Donnelly, N.J.; Randall, C.A. Refined Model of Electromigration of Ag/Pd Electrodes in Multilayer PZT Ceramics Under Extreme Humidity. *J. Am. Ceram. Soc.* **2009**, *92*, 405–410. [[CrossRef](#)]
36. Jacob, K.T.; Saji, V.S. Interaction between Ni/NiO and PbTiO₃: Phase Reversal with Redox Switching. *J. Phase Equilibria Diffus.* **2006**, *27*, 456–461. [[CrossRef](#)]

37. Florian, H.; Reichmann, K.; Kainz, G. Piezoactuator and method for the production thereof. US Patent US7,304,414, 4 December 2007.
38. Takayama, Y.; Donnelly, N.J.; Randall, C.A. Piezoelectric Actuators with Cu Inner Electrode. In Proceedings of the 13th US-Japan Seminar on Dielectric and Piezoelectric Ceramics, Hyogo, Japan, 4–7 November 2007; pp. 113–116.
39. Florian, H.; Ottlinger, M.; Sedlmaier, P. Method for Producing a Multilayer Ceramic Component. US patent US8,776,364 B2, 15 July 2014.
40. Piezo Actuators for Fuel Injection Systems—Most Reliable and Cost-efficient. Available online: <http://en.tdk.eu/tdk-en/373562/tech-library/articles/applications-cases/applications-cases/most-reliable-and-cost-efficient/1039300> (accessed on 21 November 2015).
41. Polotai, A.V.; Yang, G.Y.; Dickey, E.C.; Randall, C.A. Utilization of Multiple-Stage Sintering to Control Ni Electrode Continuity in Ultrathin Ni-BaTiO₃ Multilayer Capacitors. *J. Am. Ceram. Soc.* **2007**, *90*, 3811–3817.
42. Opitz, M.R.; Albertsen, K.; Beeson, J.J.; Hennings, D.F.; Routbort, J.L.; Randall, C.A. Kinetic Process of Reoxidation of Base Metal Technology BaTiO₃-based Multilayer Capacitors. *J. Am. Ceram. Soc.* **2003**, *86*, 1879–1884. [CrossRef]
43. Pithan, C.; Hennings, D.; Waser, R. Progress in the Synthesis of Nanocrystalline BaTiO₃ Powders for MLCC. *Int. J. Appl. Ceram. Technol.* **2005**, *2*, 1–14. [CrossRef]
44. Gui, Z.L.; Wang, Y.L.; Li, L.T. Study on the Interdiffusion in Base-Metal-Electrode MLCCs. *Ceram. Int.* **2004**, *30*, 1275–1278. [CrossRef]
45. Wang, S.; Tsai, Y.; Lee, W. Study on (Ba, Ca)(Ti, Zr)O₃ Dielectric Cofired with Copper Electrode. *Jpn. J. Appl. Phys.* **2014**, *53*, 061501. [CrossRef]
46. Yamamoto, J.; Kawano, N.; Arashi, T.; Sato, A.; Nakano, Y.; Nomura, T. Reliability of Multilayer Ceramic Capacitors with Nickel Electrodes. *J. Power Sources* **1996**, *60*, 199–203. [CrossRef]
47. Randall, C.A. Scientific and Engineering Issues of the State-of-the-Art and Future Multilayer Capacitors. *J. Ceram. Soc. Jpn.* **2001**, *109*, S2–S6. [CrossRef]
48. Yang, G.Y.; Lee, S.I.; Liu, Z.J.; Anthony, C.J.; Dickey, E.C.; Liu, Z.K.; Randall, C.A. Effect of Local Oxygen Activity on Ni-BaTiO₃ Interfacial Reactions. *Acta Mater.* **2006**, *54*, 3513–3523. [CrossRef]
49. RoHS Compliance Guide: Regulations, 6 Substances, Exemptions, WEEE. Available online: <http://www.rohsguide.com/> (accessed on 11 October 2015).
50. Directive 2011/65/EU of the European Parliament and of the Council of 8 June 2011 on the Restriction of the Use of Certain Hazardous Substances in Electrical and Electronic Equipment. Available online: <http://eur-lex.europa.eu/legal-content/EN/TXT/HTML/?uri=CELEX:32011L0065&from=EN> (accessed on 25 October 2015).
51. Egerton, L.; Dillon, D.M. Piezoelectric and Dielectric Properties of Ceramics in the System Potassium-Sodium Niobate. *J. Am. Ceram. Soc.* **1959**, *42*, 438–442. [CrossRef]
52. Saito, Y.; Takao, H.; Tani, T.; Nonoyama, T.; Takatori, K.; Homma, T.; Nagaya, T.; Nakamura, M. Lead-free Piezoceramics. *Nature* **2004**, *432*, 84–87. [CrossRef] [PubMed]
53. Guo, Y.; Kakimoto, K.; Ohsato, H. Dielectric and Piezoelectric Properties of Lead-free (Na_{0.5}K_{0.5})NbO₃-SrTiO₃ Ceramics. *Solid State Commun.* **2004**, *129*, 279–284. [CrossRef]
54. Guo, Y.; Kakimoto, K.; Ohsato, H. (Na_{0.5}K_{0.5})NbO₃-LiTaO₃ Lead-free Piezoelectric Ceramics. *Mater. Lett.* **2005**, *59*, 241–244. [CrossRef]
55. Hollenstein, E.; Davis, M.; Damjanovic, D.; Setter, N. Piezoelectric Properties of Li- and Ta-modified (K_{0.5}Na_{0.5})NbO₃ Ceramics. *Appl. Phys. Lett.* **2005**, *87*, 182905. [CrossRef]
56. Kim, M.S.; Jeong, S.J.; Song, J.S. Electromechanical Properties of NKN-5LT Multilayer Actuator. *Adv. Mater. Res.* **2007**, *26–28*, 263–266. [CrossRef]
57. Kim, M.S.; Jeon, S.; Lee, D.S.; Jeong, S.J.; Song, J.S. Lead-free NKN-5LT Piezoelectric Materials for Multilayer Ceramic Actuator. *J. Electroceramics* **2009**, *23*, 372–375. [CrossRef]
58. Kobayashi, K.; Doshida, Y.; Mizuno, Y.; Randall, C.A. Possibility of Cofiring a Nickel Inner Electrode in a (Na_{0.5}K_{0.5})NbO₃-LiF Piezoelectric Actuator. *Jpn. J. Appl. Phys.* **2013**, *52*, 1–5. [CrossRef]
59. Kawada, S.; Kimura, M.; Higuchi, Y.; Takagi, H. (K_{0.5}Na_{0.5})NbO₃-Based Multilayer Piezoelectric Ceramics with Nickel Inner Electrodes. *Appl. Phys. Express* **2009**, *2*, 111401. [CrossRef]

60. Kawada, S.; Kimura, M.; Hayashi, H.; Ogiso, K.; Konoike, T.; Takagi, H. Study of Nickel Inner Electrode Lead-free Piezoelectric Ceramics. In Proceedings of the 2011 International Symposium on Applications of Ferroelectrics and 2011 International Symposium on Piezoresponse Force Microscopy and Nanoscale Phenomena in Polar Materials (ISAF/PFM), Vancouver, BC, Canada, 24–27 July 2011.
61. Liu, C.; Liu, P.; Kobayashi, K.; Qu, W.; Randall, C.A. Enhancement of Piezoelectric Performance of Lead-Free NKN-Based Ceramics via A High-Performance Flux-NaF-Nb₂O₅. *J. Am. Ceram. Soc.* **2013**, *96*, 3120–3126. [CrossRef]
62. Wang, X.; Wu, J.; Xiao, D.; Zhu, J.; Cheng, X.; Zheng, T.; Zhang, B.; Lou, X.; Wang, X. Giant Piezoelectricity in Potassium-Sodium Niobate Lead-free Ceramics. *J. Am. Chem. Soc.* **2014**, *136*, 2905–2910. [CrossRef] [PubMed]
63. Zhang, S.; Xia, R.; Shrout, T.R.; Zang, G.; Wang, J. Characterization of Lead Free (K_{0.5}Na_{0.5})NbO₃-LiSbO₃ Piezoceramic. *Solid State Commun.* **2007**, *141*, 675–679. [CrossRef]
64. Lévêque, G.; Marchet, P.; Levassort, F.; Tran-Huu-Hue, L.P.; Ducle, J.R. Lead Free (Li,Na,K)(Nb,Ta,Sb)O₃ Piezoelectric Ceramics: Influence of Sintering Atmosphere and ZrO₂ Doping on Densification, Microstructure and Piezoelectric Properties. *J. Eur. Ceram. Soc.* **2011**, *31*, 577–588. [CrossRef]
65. Matsubara, M.; Yamaguchi, T.; Sakamoto, W.; Kikuta, K.; Yogo, T.; Hirano, S. Processing and Piezoelectric Properties of Lead-Free (K,Na) (Nb,Ta)O₃ Ceramics. *J. Am. Ceram. Soc.* **2005**, *88*, 1190–1196. [CrossRef]
66. Kobayashi, K.; Doshida, Y.; Mizuno, Y.; Randall, C.A. A Route Forwards to Narrow the Performance Gap between PZT and Lead-free Piezoelectric Ceramic with Low Oxygen Partial Pressure Processed (Na_{0.5}K_{0.5})NbO₃. *J. Am. Ceram. Soc.* **2012**, *95*, 2928–2933. [CrossRef]
67. Shimizu, H.; Kobayashi, K.; Mizuno, Y.; Randall, C.A. Advantages of Low Partial Pressure of Oxygen Processing of Alkali Niobate: NaNbO₃. *J. Am. Ceram. Soc.* **2014**, *97*, 1791–1796. [CrossRef]
68. Shigemi, A.; Wada, T. Enthalpy of Formation of Various Phases and Formation Energy of Point Defects in Perovskite-type NaNbO₃ by First-principles Calculation. *Jpn. J. Appl. Phys.* **2004**, *43*, 6793–6798. [CrossRef]
69. Shigemi, A.; Wada, T. Evaluations of Phases and Vacancy Formation Energies in KNbO₃ by First-Principles Calculation. *Jpn. J. Appl. Physics* **2005**, *44*, 8048–8054. [CrossRef]
70. Gao, R.; Chu, X.; Huan, Y.; Zhong, Z.; Wang, X.; Li, L. Ceramic-Electrode inter-Diffusion of (K, Na)NbO₃-Based Multilayer Ceramics with Ag_{0.7}Pd_{0.3} Electrode. *J. Eur. Ceram. Soc.* **2015**, *35*, 389–392. [CrossRef]
71. Kobayashi, K.; Randall, C.A. New Opportunity in Alkali Niobate Ceramics Processed in Low Oxygen Partial Pressure. In Proceedings of the Applications of Ferroelectrics held jointly with 2012 European Conference on the Applications of Polar Dielectrics and 2012 International Symp Piezoresponse Force Microscopy and Nanoscale Phenomena in Polar Materials (ISAF/ECAPD/PFM), Aveiro, Portugal, 9–13 July 2012.
72. Liu, C.; Liu, P.; Kobayashi, K.; Randall, C.A. Base Metal Co-fired (Na, K)NbO₃ Structures with Enhanced Piezoelectric Performance. *J. Electroceramics* **2014**, *32*, 301–306. [CrossRef]
73. Sapper, E.; Gassmann, A.; Gjødvad, L.; Jo, W.; Granzow, T.; Rödel, J. Cycling Stability of Lead-free BNT-8BT and BNT-6BT-3KNN Multilayer Actuators and Bulk Ceramics. *J. Eur. Ceram. Soc.* **2014**, *34*, 653–661. [CrossRef]
74. Yesner, G.; Kuciej, M.; Safari, A. Low Temperature Sintering of Bi_{0.5}Na_{0.5}TiO₃ Based Ceramics. In Proceedings of the 2015 Joint IEEE International Symposium on the Applications of Ferroelectric, International Symposium on Integrated Functionalities and Piezoelectric Force Microscopy Workshop (ISAF/ISIF/PFM), Singapore, 24–27 May 2015; pp. 21–23.
75. Masia, S.; Calvert, P.; Rhine, W.; Bowen, H. Effect of Oxides on Binder Burnout during Ceramics Processing. *J. Mater. Sci.* **1989**, *24*, 1907–1912. [CrossRef]
76. Liau, L.C.K.; Yang, T.C.K.; Viswanath, D.S. Mechanism of Degradation of Poly(Vinyl Butyral) Using Thermogravimetry/Fourier Transform Infrared Spectrometry. *Polym. Eng. Sci.* **1996**, *36*, 2589–2600. [CrossRef]
77. Liau, L.C.K.; Viswanath, D.S. Thermal Degradation of Poly (Vinyl Butyral)/ Ceramic Composites: A Kinetic Approach. *Ind. Eng. Chem. Res.* **1998**, *37*, 49–57. [CrossRef]
78. Salam, L.A.; Matthews, R.D.; Robertson, H. Pyrolysis of Polyvinyl Butyral (PVB) Binder in Thermoelectric Green Tapes. *J. Eur. Ceram. Soc.* **2000**, *20*, 1375–1383. [CrossRef]
79. Yan, H.; Cannon, W.R.; Shanefield, D.J. Poly(Vinyl Butyral) Pyrolysis: Interactions with Plasticizer and AlN Ceramic Powder. *MRS Proc.* **1991**, *249*, 377–382. [CrossRef]

80. Yan, H.; Cannon, W.R.; Shanefield, D.J. Thermal Decomposition Behaviour of Poly(Propylene Carbonate). *Ceram. Int.* **1998**, *24*, 433–439. [[CrossRef](#)]
81. Gao, L.; Ko, S.-W.; Guo, H.; Hennig, E.; Randall, C.A. Demonstration of Copper Co-fired (Na, K)NbO₃ Multilayer Structures for Piezoelectric Applications. *J. Am. Ceram. Soc.* **2016**. in press.
82. Scott, J.F. Ferroelectrics Go Bananas. *J. Phys. Condens. Matter* **2008**, *20*, 021001. [[CrossRef](#)]



© 2016 by the authors; licensee MDPI, Basel, Switzerland. This article is an open access article distributed under the terms and conditions of the Creative Commons by Attribution (CC-BY) license (<http://creativecommons.org/licenses/by/4.0/>).